Journal of Histochemistry & Cytochemistry 2014, Vol. 62(12) 846–863

DOI: 10.1369/0022155414550163
jhc.sagepub.com
SAGE

Brightfield Proximity Ligation Assay Reveals Both Canonical and Mixed Transforming Growth Factor-β/Bone Morphogenetic Protein Smad Signaling Complexes in Tissue Sections

Kathleen C. Flanders, Christopher D. Heger, Catherine Conway, Binwu Tang, Misako Sato, Samuel L. Dengler, Paul K. Goldsmith, Stephen M. Hewitt, and Lalage M. Wakefield

Laboratory of Cancer Biology and Genetics (KCF, BT, MS, SLD, LMW); Antibody and Protein Purification Unit (CDH, PKG); and Laboratory of Pathology (CC, SMH), Center for Cancer Research, National Cancer Institute, Bethesda, MD

Summary

Transforming growth factor-β (TGF-β) is an important regulator of cellular homeostasis and disease pathogenesis. Canonical TGF-β signaling occurs through Smad2/3–Smad4 complexes; however, recent in vitro studies suggest that elevated levels of TGF-β may activate a novel mixed Smad complex (Smad2/3-Smad1/5/9), which is required for some of the pro-oncogenic activities of TGF-β. To determine if mixed Smad complexes are evident in vivo, we developed antibodies that can be used with a proximity ligation assay to detect either canonical or mixed Smad complexes in formalin-fixed paraffin-embedded sections. We demonstrate high expression of mixed Smad complexes in the tissues from mice genetically engineered to express high levels of TGF-β1. Mixed Smad complexes were also prominent in 15–16 day gestation mouse embryos and in breast cancer xenografts, suggesting important roles in embryonic development and tumorigenesis. In contrast, mixed Smad complexes were expressed at extremely low levels in normal adult mouse tissue, where canonical complexes were correspondingly higher. We show that this methodology can be used in archival patient samples and tissue microarrays, and we have developed an algorithm to quantitate the brightfield read-out. These methods will allow quantitative analysis of cell type-specific Smad signaling pathways in physiological and pathological processes. (J Histochem Cytochem 62: 846–863, 2014)

Keywords

transforming growth factor-β, Smads, proximity ligation assay, brightfield, breast cancer, development, tissue microarray

Introduction

Proteins of the transforming growth factor-β (TGF-β) superfamily are important mediators of cellular homeostasis in development and in the maintenance of normal adult physiology. Dysregulation of signaling by these proteins has been implicated in a number of disease processes including cancer, chronic fibrosis and autoimmune conditions (Blobe et al. 2000; Akhurst and Hata 2012). The superfamily comprising more than 30 ligands can be divided into three groups: TGF-βs, activins/nodals, and bone morphogenetic proteins (BMPs)/growth and differentiation factors (GDFs) (Hinck 2012; Wakefield and Hill 2013). Signaling is initiated by receptor binding of ligand, which induces the formation of a heterotetrameric type II-type I receptor complex. There are numerous type I and type II receptors (RI and RII, respectively) and binding of different

Received for publication May 12, 2014; accepted July 18, 2014.

Corresponding Author:
Kathleen C. Flanders, LCBG/NCI/NIH, 37 Convent Dr, Bldg 37/Rm 5046B, Bethesda, MD 20892, USA.
E-mail: flanderk@mail.nih.gov

superfamily ligands brings together different RI-RII complexes (Shi and Massague 2003). Both RI and RII are Serine/Threonine kinases, and RI phosphorylates receptor-regulated Smads (R-Smads), which are involved in mediating downstream signal transduction (Feng and Derynck 2005). Generally TGF-βs, activins and nodals phosphorylate Smad2 or Smad3 (hereafter Smad2/3), whereas BMPs and GDFs phosphorylate Smad1, Smad5, or Smad9, previously referred to as Smad 8 (hereafter, Smad1/5/9). Phospho-R-Smads form a complex with the common mediator Smad (Smad4) and travel to the nucleus where they bind to distinct promoter elements to regulate gene transcription. Broadly speaking, TGF-βs induce formation of Smad2-Smad4 or Smad3-Smad4 complexes, which activate TGF-β response genes, whereas BMPs induce formation of Smad1-Smad4, Smad5-Smad4 or Smad9-Smad 4 complexes, which bind to a different promoter sequence to activate BMP response genes (Feng and Derynck 2005; Wakefield and Hill 2013). These pathways are referred to as the canonical "TGF-β–Smad" and "BMP–Smad" pathways, respectively.

This simplified view of TGF-β signaling has been complicated by the observation that in vitro TGF-β can sometimes phosphorylate the "BMP Smads" (Smad1/5/9) in a number of cell types, including endothelial cells, fibroblasts and normal and tumor-derived epithelial cells (Bharathy et al. 2008; Goumans et al. 2002; Wrighton et al. 2009). This unexpected phosphorylation pattern occurs when an alternate RI is recruited into the RI-RII receptor complex. Increased TGF-β expression or activation is a feature of many pathological states, including fibrosis and tumorigenesis (Blobe et al. 2000; Akhurst and Hata 2012). Interestingly, one study (Daly et al. 2008) showed that, in a variety of cultured cells, treatment with higher doses of TGF-β (~2 ng/ml) can induce the formation of a novel mixed Smad complex, whereas canonical TGF-β Smad complexes form at lower ligand concentrations. This mixed Smad complex consists of phospho-Smad2 or -3 bound to phospho-Smad1, -5, or -9 and is devoid of Smad4. In that study, mixed Smad complexes were found to mediate TGF-β-induced anchorage-independent growth in tumorigenic EpRas murine mammary epithelial cells, whereas canonical TGF-β Smad complexes mediated TGF-β-induced growth inhibition in EpH4 normal murine mammary epithelial cells. This in vitro analysis suggests that the ability of TGF-β to induce Smad1/5/9 phosphorylation may contribute to transformation. In support of this concept, TGF-β-induced phosphorylation of Smad1/5 is essential to TGF-β-induced migration and invasion in a number of tumorigenic cell lines (Bharathy et al. 2008; Liu et al. 2009)

Whereas mixed Smad complexes have been detected in vitro, it is not known if they are formed in vivo and what role they may play in TGF-β signaling in physiological or pathological processes. Standard immunohistochemical techniques that detect single proteins are insufficient to differentiate between the formation of canonical Smad and mixed Smad complexes in vivo. To examine Smad complex formation, we have used a proximity ligation assay (PLA), which allows for the detection of protein-protein interactions in tissues with subcellular resolution (Soderberg et al. 2006; Weibrecht et al. 2010). In this assay, target proteins are detected by antibodies that bring into proximity DNA strands coupled to the antibodies only when the target proteins are bound together in a complex. These antibody-bound oligonucleotides (a (+) strand and a (-) strand) can be circularized and ligated, forming immobile molecules that are amplified by rolling circle amplification (RCA). These amplification products are at the resolution of light microscopy and can be detected by binding oligonucleotides complementary to the replicated DNA strand. The complementary oligonucleotides are labeled with fluorescent molecules or with enzymes, such as peroxidase, which deposits colored products at the site of binding, enabling fluorescent or bright-field detection of the results of the assay (Weibrecht et al. 2010)

Because brightfield microscopy is used most often in routine histopathology, we developed PLA for the detection of Smad complexes with a brightfield readout as demonstrated for visualizing estradiol-estrogen receptor interactions (Zieba et al. 2010) and HER receptor dimerization (Barros et al. 2014). Brightfield microscopy offers some advantages over fluorescence microscopy as it permits counterstaining to allow simultaneous observation of tissue histopathology and generates a stable signal which can be viewed years later. In this paper, we report the generation of antibodies that allow brightfield detection of canonical Smad and mixed Smad complexes in formalin-fixed, paraffin-embedded (FFPE) sections by PLA. We use this method to identify and quantitate Smad signaling complexes in murine tissues and a breast cancer tissue microarray (TMA). Here, we demonstrate for the first time that mixed Smad complexes are indeed formed in vivo and are more prevalent in murine embryonic development and human breast cancers than in normal adult physiology.

Materials & Methods

Generation of Primary Antibodies

An antibody designed to recognize both mouse and human Smad2 and -3 was raised to the peptide sequence NPYHYQRVETP (amino acids 123–133 of Smad3), whereas an antibody designed to recognize both mouse and human Smad1, -5, and -9 was generated to the peptide sequence EFPFGSKQKEV (amino acids 110-120 of Smad1). Peptides were synthesized (AnaSpec Inc, Fremont, CA), coupled to keyhole limpet hemocyanin and injected into rabbits (Cocalico Biologics, Reamstown, PA). Antisera

Table 1. Primary Antibodies Used in This Study.

Antibody to:	Species/Clonality	Source & Product Number	Application/IgG conc. (μg/ml)
Smad1	Rb mono	Abcam (Cambridge, MA) #33902	WB (1.1)
Smad2	Rb poly	Invitrogen #51-1300	WB (2.0)
Smad3	Rb mono	Cell Signaling Technology (Beverly, MA) #9523	WB (0.08)
Smad5	Rb poly	Cell Signaling Technology #9517	WB (0.02)
β-actin	Ms mono	Sigma-Aldrich (St. Louis, MO) #A1978	WB (2.0)
Phospho-Smad2-(Ser 465/467)	Rb mono	Cell Signaling Technology #3108	WB (0.14)
			IHC (0.23)
Phospho-Smad3-(Ser 423/425)	Rb mono	Abcam # 52903	WB (0.03)
			IHC (0.3)
Phospho-Smad1/5-(Ser 463/465)- Smad9(Ser 426/428)	Rb poly	Cell Signaling Technology #9511	WB (0.08)
			IHC (0.16)
Smad4	Ms mono	Abcam #3219	PLA (4.0)
Smad1/5/9	Rb poly	In house	IS (0.01)
			PLA (1.0)
Smad2/3	Rb poly	In house	IS (0.07)
			PLA (1.0)

IHC, immunohistochemistry; IS, immunostaining; Ms, mouse; mono, monoclonal; poly, polyclonal; PLA, proximity ligation assay; Rb, rabbit; WB, western blot

were affinity purified against the immunizing peptide followed by gel filtration for further purification and buffer exchange and stored in PBS/0.1% NaN_3 at 4C.

Characterization of Primary Antibodies by Immunostaining

MDA-MB-231 cells were infected with viral media from 293T cells transfected with lentiviral vectors expressing either Smad1or -3. Following selection with 0.5 mg/ml geneticin (Life Technologies, Grand Island, NY) for 5 days, cell lysates were prepared in MPER buffer (Thermo Fisher Scientific, Waltham, MA) for western blotting, or cells were washed, scraped and centrifuged into pellets, which were fixed overnight in 10% neutral-buffered formalin (NBF) for use in immunostaining. After several washes in 70% EtOH, cell pellets were embedded in paraffin and sectioned onto polylysine-coated slides. Smad expression was decreased by reverse transfection of Smad-specific siRNAs into MDA-MB-231 cells using Lipofectamine RNAiMAX reagent (Invitrogen, Grand Island, NY) for 72 hr following the manufacturer's instructions. A pool of siRNAs that targeted both Smad2 and -3 (human) and a control siRNA were obtained from Santa Cruz Biotechnology (Dallas, TX). Human Smad1 and -5 siGenome SMARTpool siRNAs, as well as a non-targeting siRNA pool, were from Thermo Fisher Scientific. Cell lysates were prepared and other cells were centrifuged, fixed and sectioned as described above. Increased or decreased expression of Smad protein was confirmed by western blotting of the cell lysates and probing the blots with commercial antibodies for Smad1, -2, -3, -5 and β-actin (see Table 1).

Following dewaxing and antigen retrieval (described below), cell pellet sections were incubated for 2 hr at room temperature with anti-Smad2/3 (0.07 μg/ml) or anti-Smad1/5/9 (0.01 μg/ml). Immune complexes were detected using a Vectastain Elite Peroxidase Rabbit ABC kit (Vector Laboratories, Burlingame, CA) and liquid DAB concentrated substrate pack (BioGenex, San Ramon, CA) as previously described (Figueroa et al. 2010).

Treatment of MDA-MB-231 Cells with Growth Factors

Cells were grown to 90% confluence and incubated overnight in media containing reduced levels (0.2%) of fetal bovine serum. Cells were treated for 1 hr with 5 ng/ml TGF-β1 or 50 ng/ml BMP2 (both from R&D Systems, Minneapolis, MN) and then lysed in MPER buffer. Cell lysates were analyzed by western blotting for pSmad2, pSmad3, and p Smad1/5/9 (Table 1).

Tissue Sections

Paraffin sections were cut at 5 μm onto positively-charged slides. Mouse embryos were harvested at 15–16 days gestation and fixed overnight in 10% NBF. After washing in 70% ethanol, the embryos were then processed and embedded in paraffin. Mouse salivary glands or kidneys overexpressing TGF-β1 were kindly provided by Ashok Kulkarni, NIH (Hall et al. 2010) and Jeffrey Kopp, NIH (Mozes et al. 1999), respectively. Tumor xenografts were generated by implanting human breast cancer cell lines (1×10^5 cells/site for MDA-MB-231 cells and 5×10^5 cells/site for MCF-7

cells) into the 4th mammary fat pad of nude mice. MCF7 tumors were generated in ovariectomized mice and implanted with slow-release estradiol pellets (1.7 mg) from Innovative Research (Novi, MI). Tumors were harvested after 5 weeks for MDA-MB-231 cells and after 10 weeks for MCF7 cells, fixed in NBF, embedded, sectioned and used for conventional immunohistochemistry and PLA. All animal experiments were approved by the appropriate Institutional Animal Care and Use Committee. Unstained sections of an estrogen receptor (ER)-negative, lymph node-positive, grade 2 breast cancer and matched adjacent normal tissue from the same patient were purchased from Capital Biosciences (Rockville, MD). A validation breast cancer tissue microarray was obtained from the Tissue Array Research Program (TARP, NCI).

Labeling of Primary Antibodies

Solutions of anti-Smad2/3 and anti-Smad1/5/9 were concentrated to 1 mg/ml and exchanged into PBS using Vivaspin 500 5K MWCO disposable ultrafiltration devices (GE Healthcare, Piscataway, NJ). Anti-Smad2/3 and anti-Smad1/5/9 (20 μg each) were conjugated overnight to an activated PLUS oligonucleotide or activated MINUS oligonucleotide, respectively, via Lightning-Link technology using the Duolink II Probemaker kit (Olink Biosciences, Uppsala, Sweden) as directed by the manufacturer. Following addition of the stop reagent, the oligo-conjugated antibodies were placed in storage solution provided with the kit and stored at 4C.

Proximity Ligation Assay

FFPE sections were dewaxed in xylene and hydrated through an ethanol gradient. Antigen retrieval was performed in 1 mM EDTA, pH 8.0 for 10 min at 95C in an EZ Retriever (BioGenex). After an additional 10 min in the antigen retrieval solution, slides were transferred to room temperature water and sections were delimited with a Dako Pen (Dako, Glostrup, Denmark). The PLA was performed using reagents provided in a Duolink II in situ Brightfield kit (Olink Biosciences) prepared according to the manufacturer's instructions. After blocking endogenous peroxidase (5 min at room temperature) and non-specific protein binding (1 hr at 37C), sections were incubated overnight at 4C with primary antibody. Antibody pairs used were as follows: for canonical TGF-β-Smad complexes, anti-Smad 4 with anti-Smad2/3; for canonical BMP-Smad complexes, anti-Smad4 with anti-Smad1/5/9; for mixed Smad complexes, anti-Smad2/3(-) with anti-Smad1/5/9(+) (Table 1). To detect canonical Smad complexes, mouse PLUS and rabbit MINUS secondary PLA antibodies were prepared and used according to the manufacturer's instructions. Uncomplexed Smads were detected with anti-Smad2/3 or anti-Smad1/5/9 followed by incubation with rabbit PLUS and rabbit MINUS PLA secondary antibodies. The ligation and amplification reactions were carried out on all slides as described by the manufacturer. The single stranded RCA probes were visualized by reaction with an HRP-labeled hybridization probe followed by NovaRED detection for 10 min. Following 2 water washes, sections were then counterstained for 30 sec in a 1:10 dilution of QS hematoxylin (Vector Laboratories). Following a 1 min rinse in still tap water, sections were dehydrated (2×1 min in 95% ethanol; 2×1 min in 100% ethanol) before being transferred to xylene and coverslipped. Images were captured using a Zeiss Axioimager 2ie with an AxioCam HRC and Axiovision software ver 4.1 (Zeiss Microimaging; Thornwood, NY).

Blocking of PLA Signal

Aliquots of anti-Smad2/3 and anti-Smad1/5/9 diluted to working concentrations were incubated overnight at 4C with 100-fold molar excess of immunizing peptide and used as negative controls for single antibody detection. When detecting mixed Smad complexes, omission of one of the primary antibodies abolished the signal. Detection of Smad2/3-Smad 4 complexes was blocked by inclusion of the Smad2/3 peptide, as described above. The simple addition of the Smad1/5/9 peptide was not sufficient to block detection of the Smad1/5/9-Smad 4 complexes. To accomplish this, aliquots of anti-Smad1/5/9 diluted to working concentrations were incubated overnight at 4C with either resin coupled to the immunizing peptide or resin coupled to an unrelated peptide. The antibody was recovered by centrifugation and depleted anti-Smad1/5/9 (negative control) or undepleted anti-Smad1/5/9 (positive control) was combined with Smad4 for complex detection.

Quantitation of Brightfield Signals

TMA slides were digitized at 40× magnification utilizing the NanoZoomer high-throughput scanner (Hamamatsu Corp.; Bridgewater, NJ) and images were viewed using Digital Image Hub (Leica Biosystems, Wetzlar, Germany). Automated image analysis was performed utilizing TissuemorphDP analysis solution (Visiopharm, Hoersholm, Denmark). Regions were manually annotated for selection of tumor, and an algorithm was trained to capture the following steps: (1) All cells within the tumor annotated regions were isolated; (2) All possible pixels that could have potentially been an RCA amplicon were identified; (3) Based on size and color thresholding, only positive signals were isolated and included in the image analysis output. An overlay mask was created to highlight the tumor cells as green; all pixels that were counted as amplicons as pink; and all pixels, which were discounted based on thresholding

as not a true signal, as blue. The data generated from the image analysis included count of tumor cells and a count of positive amplicons.

Results

Generation and Characterization of Smad Antibodies

The Smad complexes that we were interested in detecting in vivo are shown in Figure 1A. The mixed Smad complex, which is generated by a TGF-β/BMP hybrid receptor, has been shown to form in vitro when cells are treated with more than 2 ng/ml TGF-β (Daly et al. 2008). Because the specific composition of the mixed Smad complex might vary with context, we searched for antibodies that would recognize Smad2 and -3 (TGF-β-activated Smads) or Smad1, -5, and -9 (BMP-activated Smads) such that complexes involving any combination of a TGF-β Smad with a BMP Smad could be detected. We were unable to identify commercial antibodies that detected the desired Smads in FFPE sections; so, we generated antibodies to the peptide sequences shown in Figure 1B. Sequences were chosen in regions of the MH1 domains that are conserved within the Smad class (TGF-β Smad vs BMP Smad) (Fig. 1C) and the antibodies are predicted to recognize both human and mouse Smad proteins. Although the antibodies recognized the expected recombinant GST-Smads on western blotting, they did not detect endogenous Smads in cell culture lysates, suggesting that their sensitivity in western blots was low (data not shown). As performance in western blots does not reliably predict performance of antibodies in immunostaining on FFPE sections (Skliris et al. 2002), we tested the antibodies by routine immunostaining approaches on FFPE sections of MDA-MB-231 cells over-expressing one of the Smad proteins. Western blots using commercially available antibodies confirmed the enhanced expression of Smad1 or -3 in these cells (Fig. 2A). Our new anti-Smad1/5/9 antibody preferentially stained cells over expressing Smad1 (a BMP Smad), whereas our anti-Smad2/3 preferentially stained cells overexpressing Smad3 (a TGF-β Smad) (Fig. 2B). Further characterization of the new antibodies was performed in MDA-MB-231 cells where siRNAs were used to knockdown Smad1/5 or Smad2/3. To knock down Smad1/5/9, two separate pools of target-specific siRNAs for Smad1 and -5 were mixed together. RT-qPCR analysis showed very low endogenous expression of Smad9 in these cells (data not shown) so the siRNA for Smad9 was not included. A substantial knockdown of Smad1 and -5 was confirmed by western blotting with commercial antibodies when siRNAs to Smad1or -5 were used either alone or in combination (Fig. 2C). For Smad2/3, a pool of target-specific siRNAs knocked down both Smad2 and -3 proteins as demonstrated by western blotting with commercial Smad2 and -3 antibodies (Fig. 2C). Cells with decreased levels of BMP-Smads or TGF-β-Smads showed decreased staining with our anti-Smad1/5/9 and anti-Smad2/3 antibodies, respectively, whereas cells expressing a non-targeting siRNA did not (Fig. 2D). Taken together, these results indicate that our anti-Smad1/5/9 and anti-Smad2/3 antibodies are detecting the expected proteins in FFPE sections.

Before looking at complex formation with the combinations of antibodies, we initially tested the anti-Smad2/3 and anti-Smad1/5/9 antibodies as single agents for the detection of Smads with brightfield PLA. Because these antibodies were raised in rabbits, rabbit-PLUS and rabbit-MINUS secondary antibodies were used to detect the signal. PLA staining of 15-day mouse embryos showed that most tissues expressed some signal for both Smad2/3 and Smad1/5/9, as previously reported (Flanders et al. 2001). The PLA signals appear as red dots (open arrowheads in Fig. 2E). The strongest expression of Smad1/5/9 was found in myocardium (Fig. 2E), as well as in endothelium, skeletal muscle, and submucosal mesenchyme of the stomach and intestine, whereas expression of Smad2/3 was strongest in the ossification centers throughout the embryo (Fig. 2E), and the epithelium of the salivary gland, lung, stomach and intestine.

Figure 1. Strategy to detect Smad signaling complexes. (A) Low levels of TGF-β ligand signal through a complex of dimeric type I and dimeric type II TGF-β receptors to phosphorylate Smad2 and -3 (the "TGF-β Smads"), which combine with Smad4 to generate the canonical TGF-β Smad signaling complex (left). In contrast, BMP ligands signal through a complex of dimeric type I and type II BMP receptors to phosphorylate Smad1, -5, and -9 (the "BMP Smads"), which combine with Smad4 to generate the canonical BMP Smad signaling complexes (right). Higher levels of TGF-β ligand can induce formation of a hybrid TGF-β/BMP receptor complex (TβRII dimer-TβRI monomer-BMP RI monomer), which phosphorylates both Smad2/3 and Smad1/5/9. These phosphorylated Smads combine in the absence of Smad 4 to generate mixed Smad complexes that contain both TGF-β Smads and BMP Smads (middle). This model is based on work of Daly et al. (2008). (B) Antibodies recognizing either TGF-β Smads or BMP Smads were raised against peptides corresponding to the indicated amino acids. (C) Sequence alignment showing that the peptide sequences chosen (boxed residues) are conserved within the given Smad subfamily, but differ significantly between them. The selected sequences are identical in both human and mouse. Identical residues are highlighted in yellow, conservative substitutions are highlighted in blue, blocks of similar residues are highlighted in green, and non-similar residues are not highlighted. Numbers above the sequence represent the amino acid number in the consensus sequence.

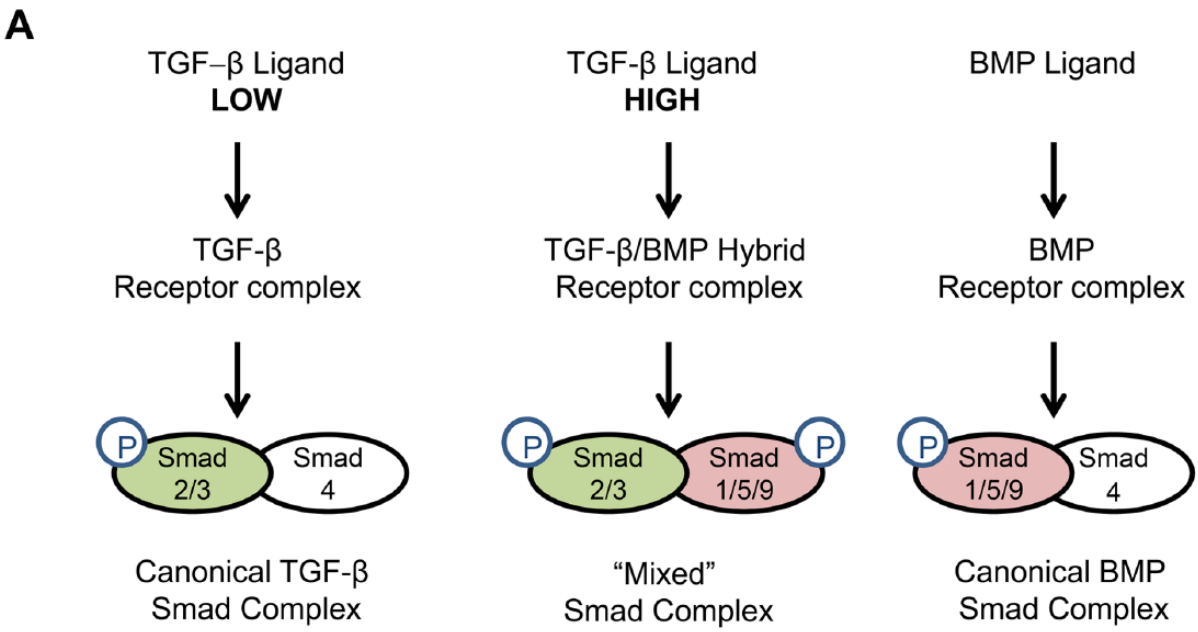
A
TGF–β Ligand
LOW
TGF-β Ligand
HIGH
BMP Ligand
TGF-β
Receptor complex
TGF-β/BMP Hybrid
Receptor complex
BMP
Receptor complex
P
Smad
2/3
Smad
4
P
Smad
2/3
Smad
1/5/9
P
P
Smad
1/5/9
Smad
4
Canonical TGF-β
Smad Complex
"Mixed"
Smad Complex
Canonical BMP
Smad Complex

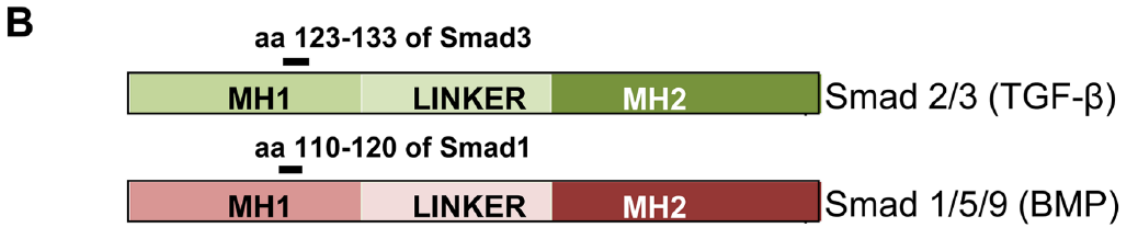
B
aa 123-133 of Smad3
MH1
LINKER
MH2
Smad 2/3 (TGF-β)
aa 110-120 of Smad1
MH1
LINKER
MH2
Smad 1/5/9 (BMP)

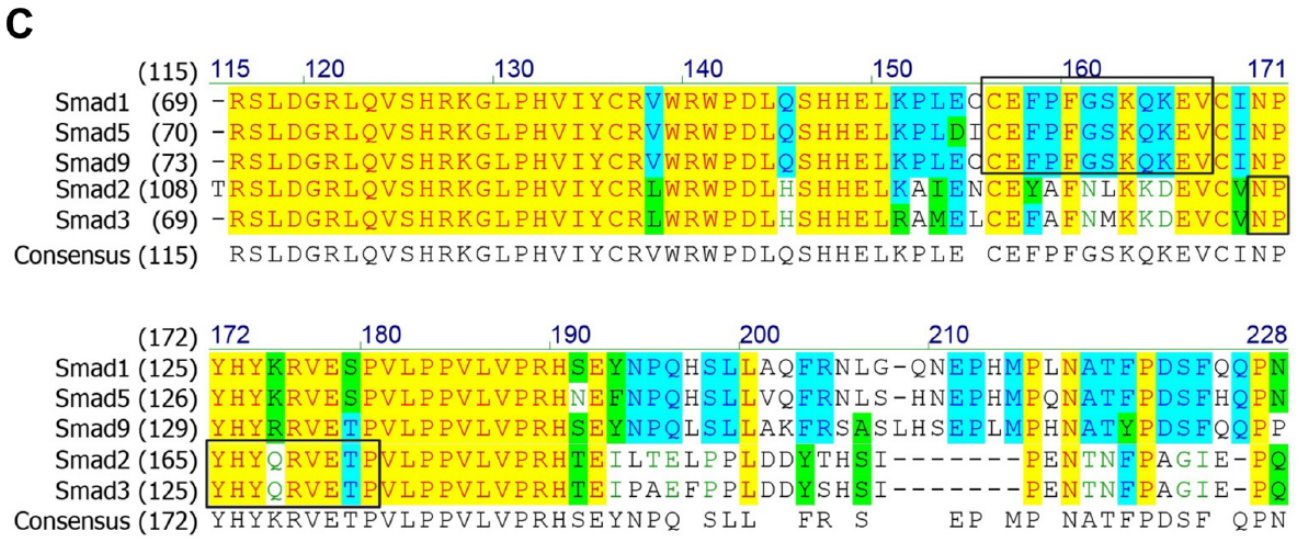
C
(115) 115 120 130 140 150 160 171
Smad1 (69) -RSLDGRLQVSHRKGLPHVIYCRVWRWPDLQSHHELKPLECCEFPFGSKQKEVCINP
Smad5 (70) -RSLDGRLQVSHRKGLPHVIYCRVWRWPDLQSHHELKPLDICEFPFGSKQKEVCINP
Smad9 (73) -RSLDGRLQVSHRKGLPHVIYCRVWRWPDLQSHHELKPLECCEFPFGSKQKEVCINP
Smad2 (108) TRSLDGRLQVSHRKGLPHVIYCRLWRWPDLHSHHELKAIENCEYAFNLKKDEVCVNP
Smad3 (69) -RSLDGRLQVSHRKGLPHVIYCRLWRWPDLHSHHELRAMELCEFAFNMKKDEVCVNP
Consensus (115) RSLDGRLQVSHRKGLPHVIYCRVWRWPDLQSHHELKPLE CEFPFGSKQKEVCINP
(172) 172 180 190 200 210 228
Smad1 (125) YHYKRVESPVLPPVLVPRHSEYNPQHSLLAQFRNLG-QNEPHMPLNATFPDSFQQPN
Smad5 (126) YHYKRVESPVLPPVLVPRHNEFNPQHSLLVQFRNLS-HNEPHMPQNATFPDSFHQPN
Smad9 (129) YHYRRVETPVLPPVLVPRHSEYNPQLSLLAKFRSASLHSEPLMPHNATYPDSFQQPP
Smad2 (165) YHYQRVETPVLPPVLVPRHTEILTELPPLDDYTHSI-------PENTNFPAGIE-PQ
Smad3 (125) YHYQRVETPVLPPVLVPRHTEIPAEFPPLDDYSHSI-------PENTNFPAGIE-PQ
Consensus (172) YHYKRVETPVLPPVLVPRHSEYNPQ SLL FR S EP MP NATFPDSF QPN

The signal was blocked when antibodies were pre-incubated with the immunizing peptide (Fig. 2E).

Development of Brightfield PLA for the Detection of Smad Complexes

To examine the formation of Smad complexes, we used tumor xenografts generated by injecting MDA-MB-231 breast cancer cells into the mammary fat pad of nude mice. First, we demonstrated in vitro that MDA-MB-231 cells treated with TGF-β showed increased phosphorylation both of the TGF-β Smads (Smad2 and -3) and the BMP Smads (Smad1 and -5) by western blotting (Fig. 3A), thus confirming the results of Daly et al. (2008). As expected, treatment of cells with BMP2 induced the expression of pSmad1/5/9 (Fig. 3A). Using immunohistochemistry, we showed that tumors generated from these MDA-MB-231 cells expressed phosphorylated Smad2/3 and Smad1/5, confirming that pathway activation was occurring in vivo as well as in vitro (Fig. 3B).

We next determined if we could detect canonical Smad complexes using PLA on tumor tissue samples. Canonical BMP- and TGF-β-induced Smad complexes (Smad1/5/9-Smad4 and Smad2/3-Smad4, respectively) were detected in these tumors (Fig. 3I, 3J) by pairing our rabbit antibodies with a mouse anti-Smad4 (Fig. 3C). The Smad complexes appeared both in the nucleus and the cytoplasm, and this was as expected, because Smad complexes form in the cytoplasm and are then transported to the nucleus (Hill 2009). Blocking of the canonical BMP Smad complex was achieved by depleting anti-Smad1/5/9 of antigen with a peptide-conjugated resin, as described in Materials & Methods (Fig. 3L). Formation of the Smad2/3-Smad4 complex in the tumors was blocked by immunizing the Smad2/3 peptide (Fig. 3M).

Having succeeded with the canonical Smad complexes, we moved onto the mixed complexes. In order to detect putative mixed Smad complexes (Smad2/3-Smad1/5/9) using our anti-Smad2/3 and anti-Smad1/5/9 antibodies, we modified the standard PLA protocol, which requires the use of antibodies from two different species (Fig. 3C), because both of our anti-Smad antibodies were raised in rabbit. We directly conjugated a PLUS oligonucleotide to anti-Smad2/3 and a MINUS oligonucleotide to anti-Smad1/5/9 using the Duolink probemaker kit (Fig. 3D). To test the detection of the mixed Smad complexes using the anti-Smad2/3 PLUS and the anti-Smad1/5/9 MINUS, we performed PLA staining on FFPE sections of MDA-MB-231 cells treated with TGF-β at a concentration (5 ng/ml) previously shown to induce formation of mixed Smad complexes in vitro (Daly et al. 2008) (Fig. 3E–3H). Cells that were transfected with a non-targeting siRNA showed a dramatic increase in the formation of mixed Smad complexes upon treatment with TGF-β (Fig. 3G) as compared with untreated cells (Fig. 3E). Cells transfected with Smad2/3 siRNA failed to show expression of mixed Smad complexes either with (Fig. 3H) or without (Fig. 3F) TGF-β treatment, which would be expected if Smad2 or -3 were a component of the mixed Smad complex. This combination of antibodies also detected mixed Smad complexes in the MDA-MB-231 breast cancer xenografts (Fig. 3K), where we also saw expression of canonical Smad complexes. Omitting one of the primary antibodies resulted in total loss of signal (Fig. 3N). Thus, using our antibodies for the PLA technique, we were able to detect endogenous levels of canonical BMP Smad, canonical TGF-β Smad and non-canonical mixed Smad complexes in FFPE tumor tissues.

Overexpression of TGF-β1 Induces Expression of Mixed Smad Complexes

In vitro data suggest that treatment of cells with higher levels of TGF-β preferentially induces the formation of mixed Smad complexes (Daly et al. 2008). To determine if this was also observed in vivo, we used two transgenic mouse models in which active TGF-β1 is over-expressed

Figure 2. Characterization of anti-Smad1/5/9 and anti-Smad2/3 antibodies. (A) Western blots using commercial antibodies to Smad1 or -3 on lysates of MDA-MB-231 cells transduced with lentiviral vectors to Smad1 (S1) or Smad3 (S3) confirm the expected overexpression of the Smads. Loading control, β-actin. (B) Formalin-fixed paraffin-embedded (FFPE) sections of MDA-MB-231 cells overexpressing Smad1 or Smad3 were immunostained with anti-Smad1/5/9 (upper) or anti-Smad2/3 (lower) using conventional peroxidase immunostaining. Note that signal was underdeveloped on these sections so that the overexpressed Smad could be visualized over the endogenous levels. Scale, 5 μm. (C) Western blots using commercial antibodies to Smad1, -2, -3, or -5 on lysates of MDA-MB-231 cells transfected with siRNAs to a non-targeting sequence (NT), Smad1 (S1) and/or Smad5 (S5), or Smad2/3 (S2/3) confirmed the knock-down of the various Smad proteins. Loading control, β-actin. (D) FFPE sections of MDA-MB-231 cells transfected with siRNAs to the NT sequence, Smad1 and -5 or Smad2/3 were immunostained with anti-Smad1/5/9 (upper) or anti-Smad2/3 (lower) antibodies using conventional peroxidase immunostaining. Scale, 5 μm. (E) Detection of individual complex components. Rolling circle amplification (RCA) products (red dots, as indicated by arrow heads) following proximity ligation assay (PLA) staining of 15-day mouse embryo myocardium with anti-Smad1/5/9 (left), or the embryo ossification centers with anti-Smad2/3 (right). For this experiment, rabbit secondary antibodies labeled with both PLUS and MINUS oligonucleotides were used to generate the signal. Inclusion of the immunizing peptide during the primary antibody incubation abolished the staining. Scale, 10 μm.

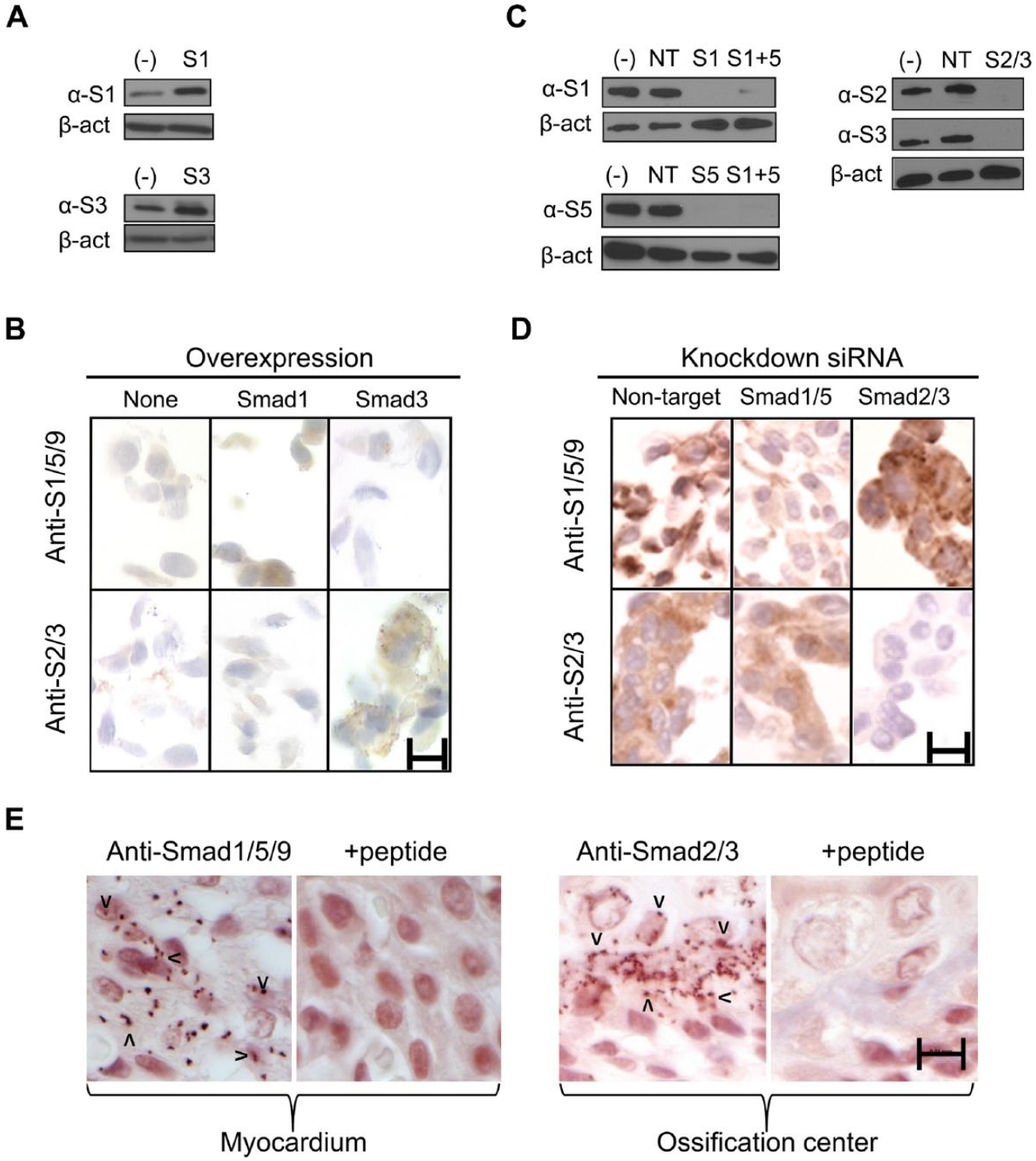
A
(-) S1
α-S1
β-act
(-) S3
α-S3
β-act
C
(-) NT S1 S1+5
α-S1
β-act
(-) NT S5 S1+5
α-S5
β-act
(-) NT S2/3
α-S2
α-S3
β-act
B
Overexpression
None
Smad1
Smad3
Anti-S1/5/9
Anti-S2/3
D
Knockdown siRNA
Non-target
Smad1/5
Smad2/3
Anti-S1/5/9
Anti-S2/3
E
Anti-Smad1/5/9
+peptide
Anti-Smad2/3
+peptide
Myocardium
Ossification center

to examine the effect of elevated TGF-β levels on Smad signaling complexes. In the first model, active TGF-β1 is conditionally expressed in the salivary gland using the Cre-Lox system. Thus, in addition to increased staining for TGF-β in the salivary glands, these mice also exhibit fibrosis and acinar atrophy (Hall et al. 2010), suggesting that the TGF-β is biologically active. Using PLA of the Smad complexes in the salivary glands from these mice, we found no change in the number of BMP Smad complexes as compared with the control (Fig. 4A, 4D) but a slight increase in canonical TGF-β Smad complexes (Fig. 4B, 4E) and a substantial increase in the mixed Smad complexes (Fig. 4C, 4F). In the second model, active TGF-β1 is under the control of regulatory elements of the mouse albumin gene, which is expressed in the liver (Sanderson et al. 1995). In these mice, the resultant increase in plasma TGF-β levels leads to severe glomerulosclerosis and an accumulation of extracellular matrix in the kidney (Mozes et al. 1999). In this model, we again observed a dramatic increase in mixed Smad complexes in the kidneys of transgenic mice (Fig. 4I, 4L) and little change in the amount of BMP Smad complexes as compared with the control (Fig. 4G, 4J). In contrast to the salivary gland, in this second model, the transgenic animals that overexpressed TGF-β showed a decreased number of canonical TGF-β Smad complexes (Fig. 4H, 4K). Conceivably, this could be due to competition between canonical and non-canonical complexes for limiting amounts of the Smad2/3 components. In each model, organs from the transgenic mice that expressed normal TGF-β levels did not demonstrate an increase in mixed Smad complexes (data not shown). The results from these two models suggest that high levels of TGF-β preferentially enhance signaling through mixed Smad complexes in vivo.

Mixed Smad Complexes Are Expressed during Murine Development

Because genetically engineered increases in TGF-β ligand in tissues resulted in enhanced mixed Smad signaling, we next wished to examine Smad complex formation in the context of naturally high TGF-β signaling. TGF-β is highly expressed during development (Heine et al. 1987; Lehnert and Akhurst 1988; Pelton et al. 1990); thus, we used 15-day mouse embryos and studied numerous tissues in a single section. We detected low levels of canonical Smad complexes in the embryo (Fig. 5A, 5B, 5D, 5E) but observed moderate numbers of mixed Smad complexes in multiple embryonic tissues, including the spinal cord (Fig. 5C), kidney (Fig. 5F), intestine, liver, brain, heart, lung, skeletal muscle, and developing bone. Furthermore, in the kidney, mixed Smad complexes were more evident in the 15-day mouse embryo (Fig. 5D–5F), whereas canonical TGF-β Smad complexes were more evident in the adult tissues (Fig. 4G–4I). Although we did not do an extensive comparison between adult and embryonic tissues with respect to the abundance of mixed versus canonical Smad complexes, our preliminary studies suggest a similar pattern in the salivary gland, liver, intestine and heart and may indicate that non-canonical mixed Smad signaling is more highly activated during embryogenesis than in normal adult tissue homeostasis, whereas the converse is true for canonical signaling.

Mixed Smad Signaling Is Induced in Breast Cancer

In detecting Smad complexes in tumor cells of MDA-MB-231 xenografts (Fig. 6D–6F), we noticed the surrounding normal mouse mammary epithelial ducts

Figure 3. Proximity ligation assay (PLA) detection of Smad complexes. (A) MDA-MB-231 cells were treated with TGF-β or BMP2 for 1 hr and pSmad2, pSmad3, or pSmad1/5/9 were detected by western blotting using commercial antibodies. Loading control, β-actin. (B) Xenograft tumors generated by injection of MDA-MB-231 cells into nude mice were stained with the antibodies used in (A) using peroxidase immunohistochemistry. Scale, 25 μm. (C) Canonical Smad complexes were detected by pairing either rabbit (Rb) anti-Smad1/5/9 (left) or anti-Smad2/3 (right) with mouse (Ms) anti-Smad4. The primary (1°) antibodies are detected by species-specific secondary (2°) antibodies coupled to either a (+) or (-) oligonucleotide that will hybridize if in close proximity. Following ligation and amplification, the rolling circle amplification (RCA) products are detected by peroxidase-conjugated oligonucleotides and detected with Nova Red. (D) Mixed Smad complexes were detected by conjugating either a (+) or (-) oligonucleotide directly onto the Rb 1° antibodies and detected as described in (C). (E–H) PLA for mixed Smad complexes in formalin-fixed, paraffin-embedded (FFPE) sections of MDA-MB-231 cells transfected with siRNAs to a non-targeting sequence (E, G) or Smad2/3 (F, H). Cells were treated with TGF-β (5 ng/ml) for 45 min (G, H) or left untreated (E, F). TGF-β induced the expression of mixed Smad complexes in cells with non-targeting siRNA (G vs E), but not in cells with Smad2/3 knockdown (H and F). Signals appear as red dots and are marked with arrowheads. Scale, 10 μm. (I–N) Canonical BMP Smad complexes (I), canonical TGF-β Smad complexes (J), and mixed Smad complexes (K) were detected in tumor xenografts generated from MDA-MB-231cells using PLA. Signals appear as red dots in both the nucleus (arrows) and cytoplasm (arrowheads). Negative controls (L–N) were performed as described in the text and showed no signal. Scale, 10 μm.

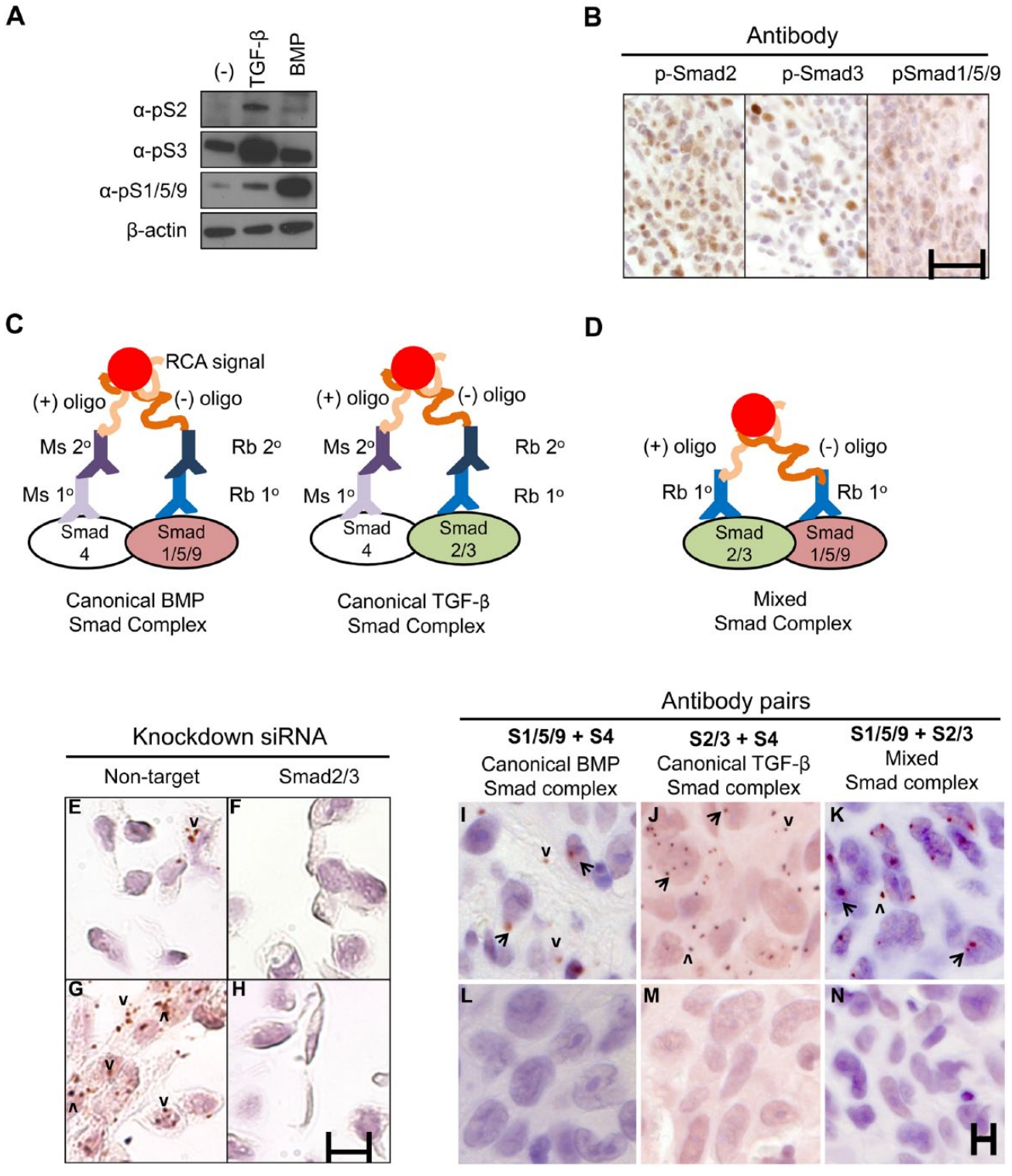
A
(-)
TGF-β
BMP
α-pS2
α-pS3
α-pS1/5/9
β-actin
B
Antibody
p-Smad2
p-Smad3
pSmad1/5/9
C
RCA signal
(+) oligo
(-) oligo
Ms 2°
Rb 2°
Ms 1°
Rb 1°
Smad 4
Smad 1/5/9
Canonical BMP Smad Complex
(+) oligo
(-) oligo
Ms 2°
Rb 2°
Ms 1°
Rb 1°
Smad 4
Smad 2/3
Canonical TGF-β Smad Complex
D
(+) oligo
(-) oligo
Rb 1°
Rb 1°
Smad 2/3
Smad 1/5/9
Mixed Smad Complex
Knockdown siRNA
Non-target
Smad2/3
E
F
G
H
Antibody pairs
S1/5/9 + S4
Canonical BMP Smad complex
S2/3 + S4
Canonical TGF-β Smad complex
S1/5/9 + S2/3
Mixed Smad complex
I
J
K
L
M
N

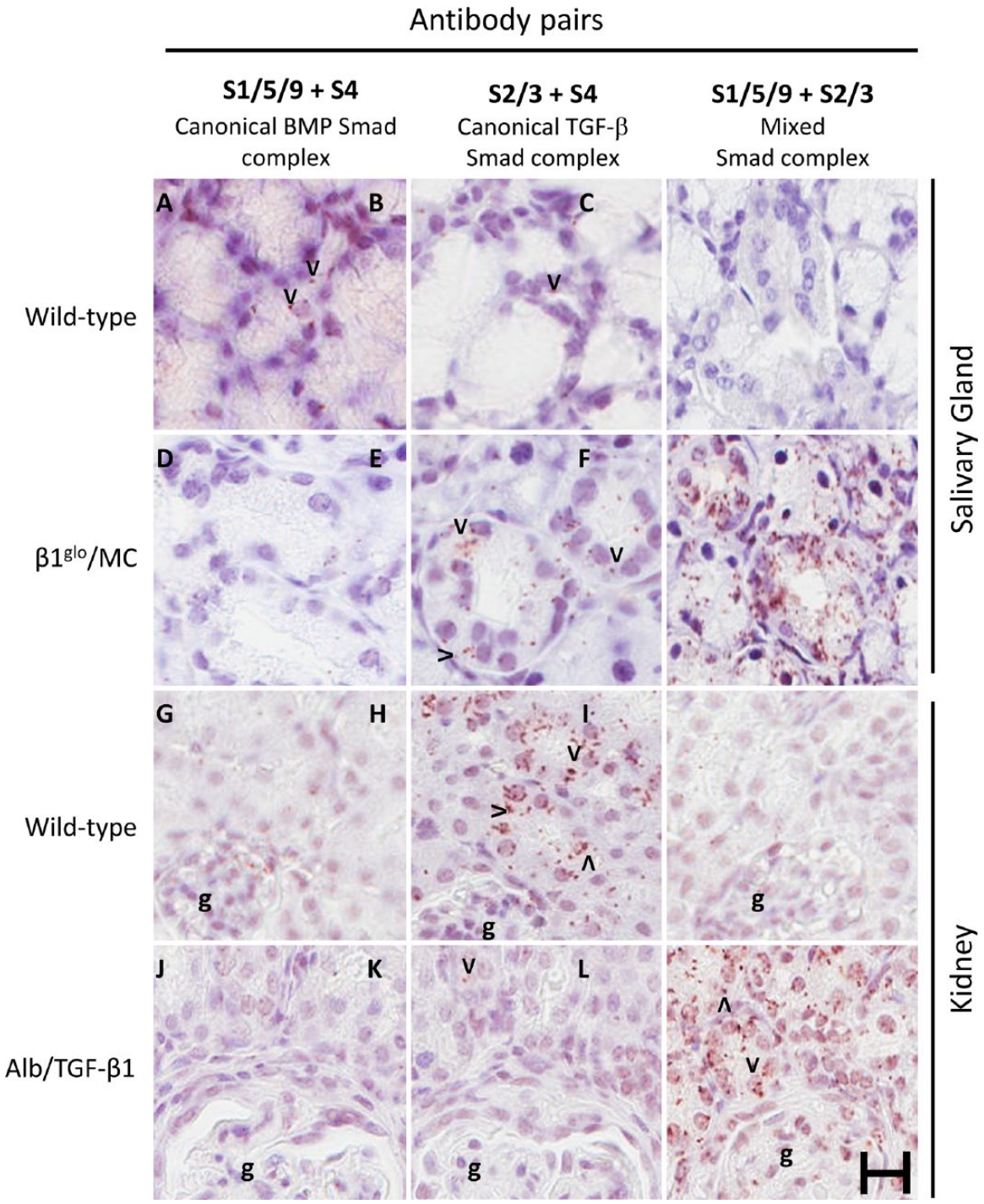

Figure 4. Signaling through mixed Smad complexes increases in tissues from transgenic mice that overexpress TGF-β1. Adult salivary glands from control mice (A–C) or mice that overexpress TGF-β1 in the salivary gland ($\beta1^{glo}$/MC) (D–F) were stained for canonical BMP-, canonical TGF-β-, or mixed Smad complexes using PLA, as described in the text. Similar staining was performed on adult kidneys from control mice (G–I) and glomerulosclerotic kidneys from mice with hepatic overexpression of TGF-β1(Alb/TGF-β1) (J–L). g, glomeruli. Arrowheads mark representative rolling circle amplification (RCA) products in panels with detectable signals. Scale, 5 μm.

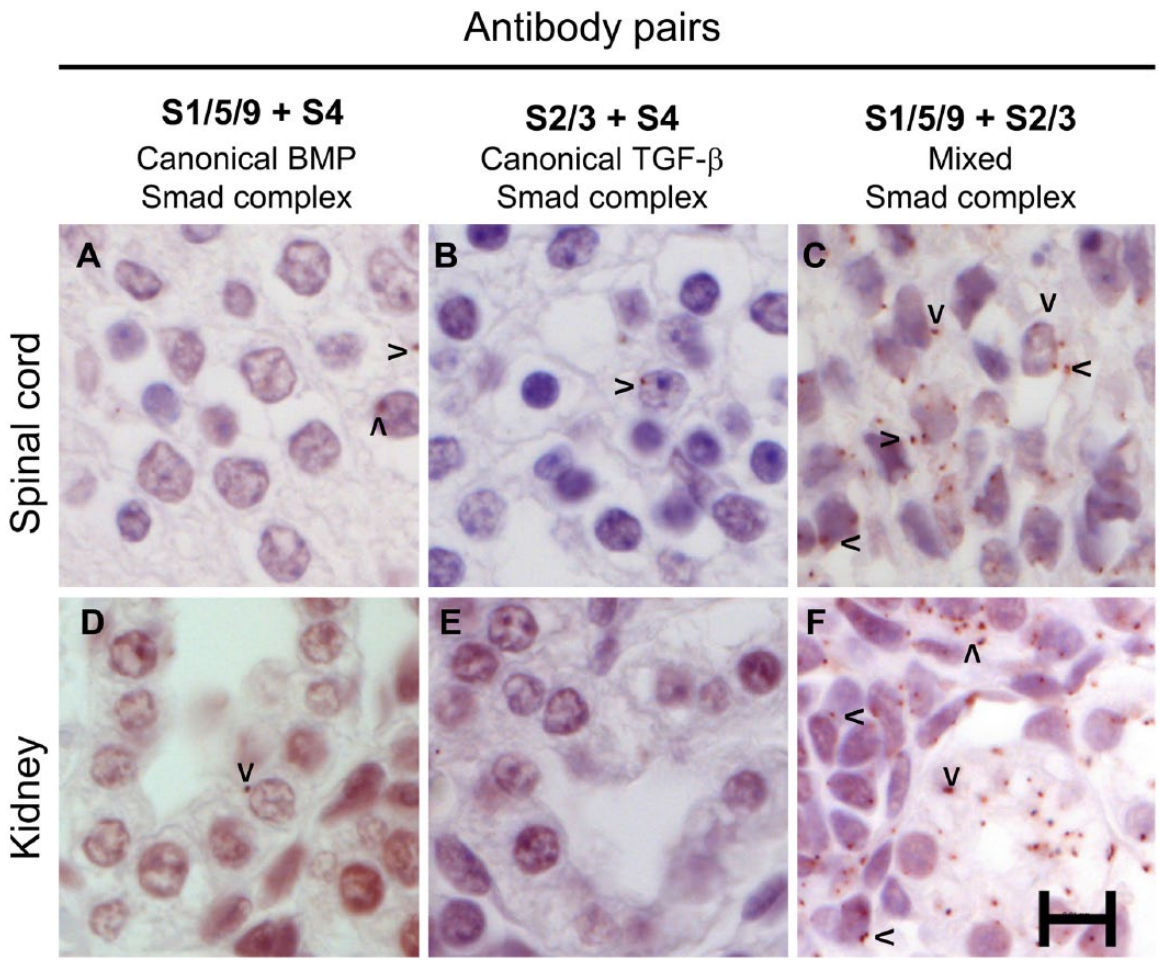

Figure 5. Expression of Smad complexes during murine development. Spinal cord (A–C) and kidney (D–F) from 15-day gestation mouse embryos were stained for canonical BMP- (A, D), canonical TGF-β- (B, E) and mixed (C, F) Smad complexes using the proximity ligation assay. Arrowheads mark some rolling circle amplification products in panels with detectable signals. Scale, 10 µm.

(Fig. 6A–6C) were devoid of expression of mixed Smad complexes (Fig. 6C), even though canonical complexes were detected (Fig. 6A, 6B). A similar pattern was seen in xenograft tumors produced by the injection of MCF-7 breast cancer cells (data not shown). We also examined Smad complexes in a human ER-, LN+ grade 2 breast cancer tissue sample and matched adjacent normal tissue sample. Although we found both canonical TGF-β Smad and mixed Smad complexes expressed in the tumor cells (Fig. 6J–6L), only canonical TGF-β Smad complexes were seen in the normal breast epithelium (Fig. 6G–6I). This suggests that, in the adult mouse and human breast, the activation of mixed Smad complexes may only occur under pathological conditions.

Detection of Smad Signaling Complexes in a Small Breast Cancer TMA

Because the above studies suggested that mixed Smad complexes were expressed higher in breast cancers than in normal breast epithelium, we examined Smad complex expression in a 90-core test breast cancer tissue microarray (TMA). We detected different patterns of Smad complex expression in numerous cores. Examples are shown in Figure 7, where each row of the panel represents the expression of one of the three Smad complexes captured from similar areas of the same core. One area of tumor cells in core 2C shows similar expression levels of canonical and mixed Smad complexes (Fig. 7A–7C). In another region of the same core, there is high expression of mixed Smad complexes in what appear to be cancer-associated fibroblasts (Fig. 7F), whereas these cells showed very little expression of canonical BMP- or TGF-β Smad complexes (Fig. 7D, 7E). Other cores showed a higher expression of canonical BMP Smad complexes (Fig. 7G) with significantly less expression of either canonical TGF-β or mixed Smad complexes (Fig. 7H, 7I). The results obtained with this breast cancer TMA demonstrate that the PLA methodology can be applied to TMAs and that breast cancers show heterogeneous expression patterns of Smad complexes.

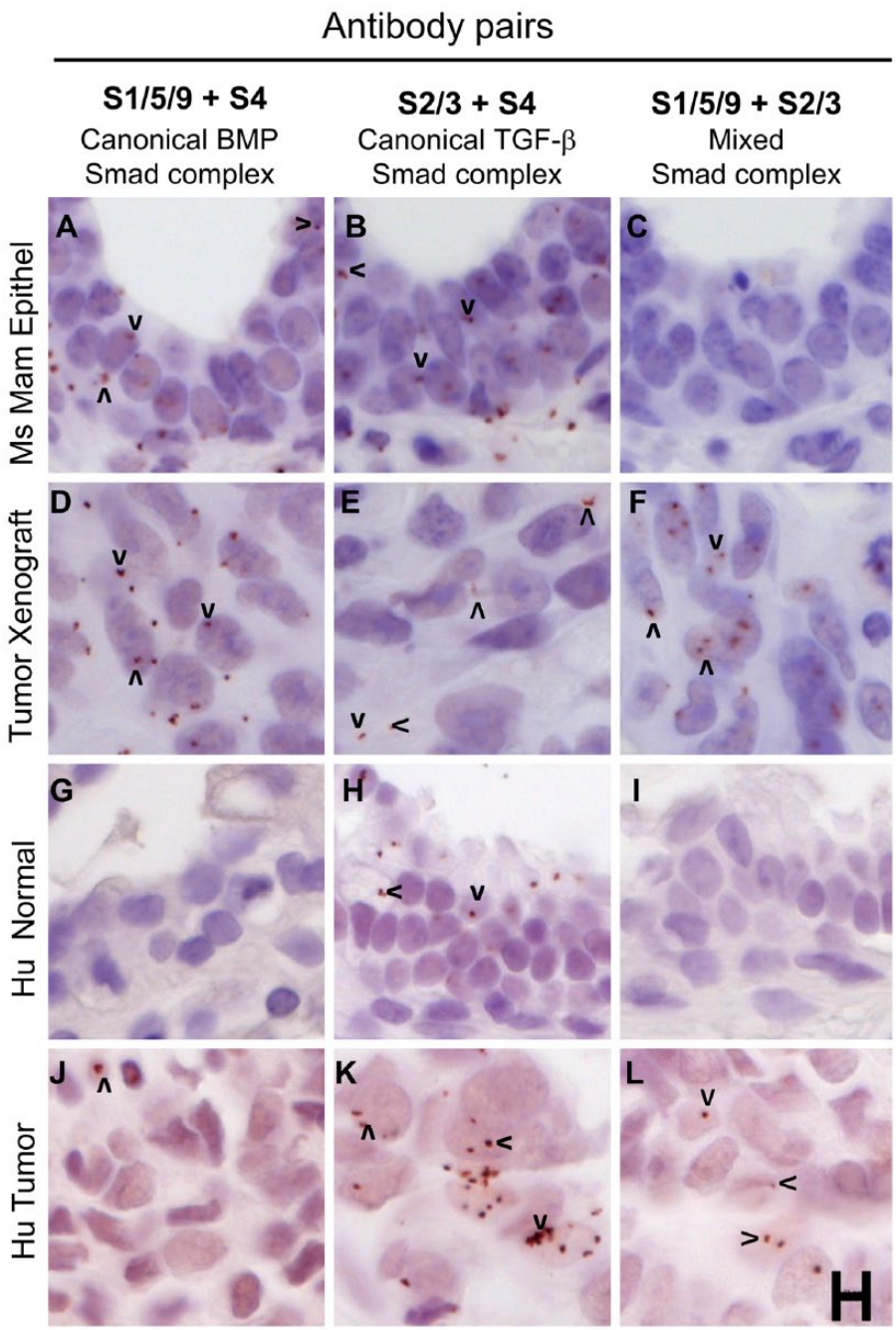

Figure 6. Mixed Smad complexes are expressed in mammary tumors but not normal mammary epithelium. (A–F) MDA-MB-231 xenograft tumors grown in the mammary fat pads of mice show expression for all three Smad complexes: (D) canonical BMP Smad, (E) canonical TGF-β Smad and (F) mixed Smad complexes, whereas mammary epithelium, with a more normal histological appearance, shows expression of canonical Smad complexes (A, B), but not mixed Smad complexes (C). (G–L) A human breast tumor shows the expression of canonical and mixed Smads (J–L) whereas normal breast tissue from the same patient expresses the canonical TGF-β Smad complexes (H) but no mixed Smad complexes (I). Arrowheads mark examples of positive rolling circle amplification (RCA) products in panels with detectable signals. Scale, 10 μm.

To facilitate the analysis of the TMAs showing expression of various Smad complexes, an image analysis algorithm was developed to recognize and quantitate the brightfield signal in each TMA core. After annotation of the part of the core containing tumor cells, the tumor cells were identified and marked in green. All possible signals that could potentially be an RCA product were identified and marked in pink. Based on size and color thresholding, some signals were discounted as not a true RCA product and these were marked in blue. The number of tumor cells and the net positive signals were quantitated for each core. The RCA products for canonical TGF-β Smad complexes of core 2D (shown in Fig. 8A) were quantitated at 2467 signals in 2394 tumor cells. The same core contained 399 signals in 2094 cells and 75 signals in 2228 cells for mixed and canonical BMP Smad complexes, respectively. Of the 90 cores present in the test TMAs, there were 73 cores in which the integrity of the tissue allowed for the quantitation of all

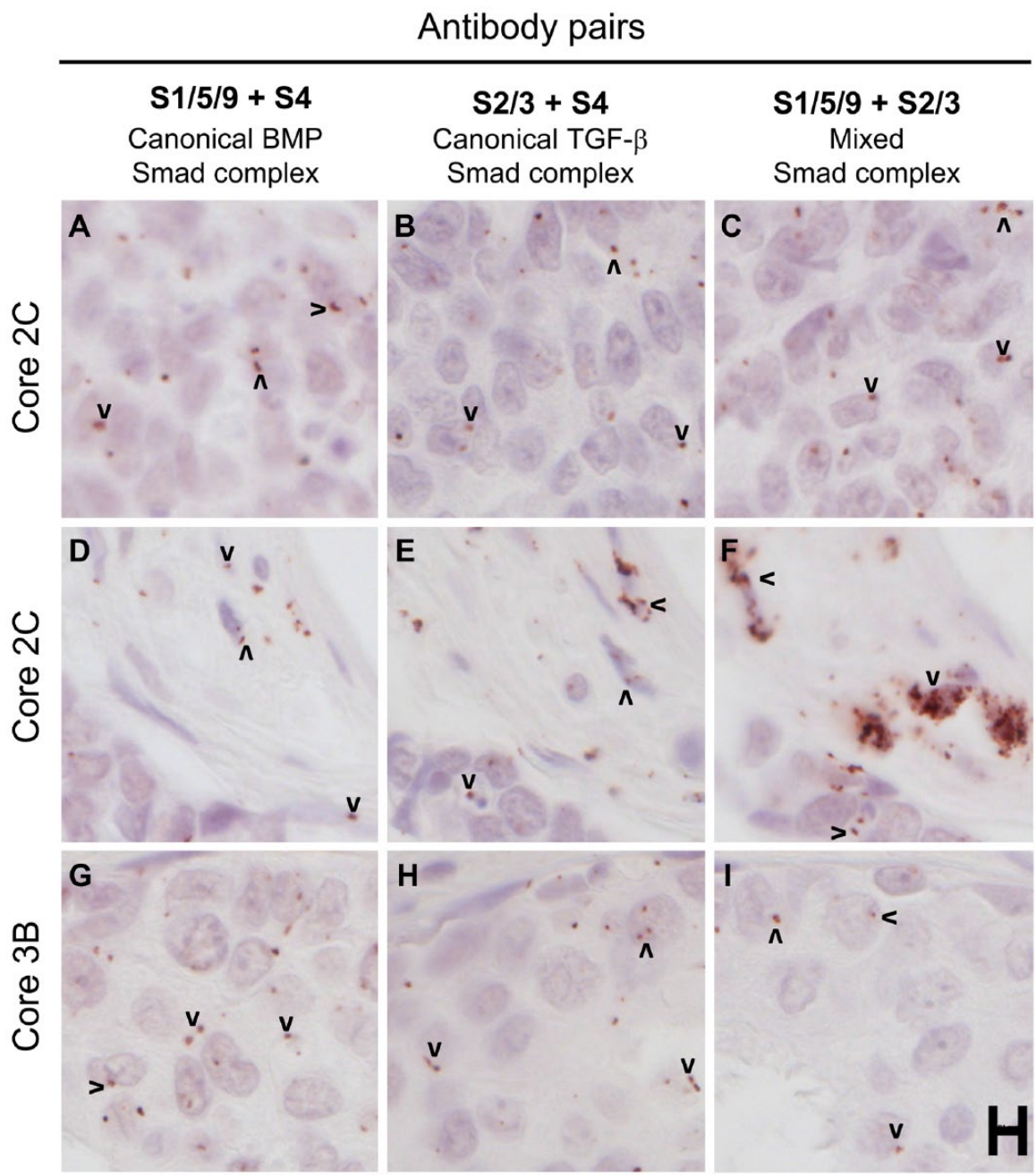

Figure 7. Human breast cancer tissues from a test tissue microarray (TMA) show different patterns of expression of Smad complexes. The proximity ligation assay was used to detect canonical BMP Smad (A, D, G), canonical TGF-β Smad (B, E, H) and mixed Smad (C, F, I) complexes in a test TMA of human breast cancer tissues. Images in each row were acquired from similar regions of the tissue cores. A–C and D–F represent two different areas of the same cores, whereas G–I are from an independent core. Arrowheads mark examples of positive rolling circle amplification (RCA) products in panels with detectable signals. Scale, 10 µm.

three Smad signaling complexes. Figure 8B shows the distribution of tumors expressing different combinations of the Smad signaling complexes when compared on a signal/cell basis. None of the cores showed signaling through mixed Smad complexes only, and the mixed Smad complexes were invariably expressed in cores that also showed detectable levels of canonical BMP- and/or TGF-β Smad complexes. A significant subset of cores expressed canonical

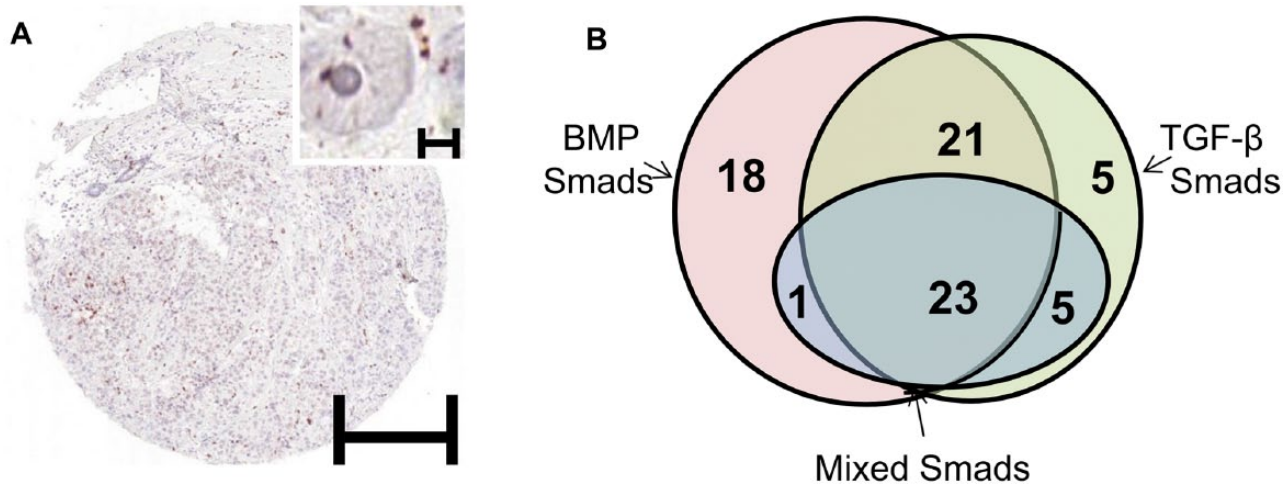

Figure 8. (A) Core 2d from test breast cancer tissue microarray (TMA) showing rolling circle amplification products for canonical TGF-β Smad complexes. Scale, 100 µm. Inset shows higher magnification of proximity ligation assay signal. Scale, 5 µm. (B) Venn diagram showing the numbers of cores in the test TMA expressing various combinations of Smad complexes.

Smad complexes without the presence of mixed Smad complexes. These different patterns of signaling suggest complex interactions between TGF-β and BMP signaling pathways in breast carcinogenesis. The breast cancer TMA lacks additional clinicopathological information, which meant that we were unable to determine the significance of these results.

Discussion

Proximity ligation assay allows for the detection of endogenous protein-protein interactions in tissue samples. This technique has the potential to support a more sophisticated analysis of signal transduction processes and cross-talk between signaling pathways in tissues than is possible by monitoring a single component. TGF-β is a central regulatory molecule in homeostasis and disease, and its pleiotropic and context-dependent activities are likely to be mediated by engagement and activation of different combinations of signaling components in different settings (Feng and Derynck 2005). Recently, high levels of TGF-β ligand, such as would be seen in pathological situations, have been shown to activate non-canonical signaling through mixed Smad complexes in vitro (Daly et al. 2008). Utilizing PLA, we show for the first time the existence of mixed Smad signaling complexes in vivo. Our in vivo studies agree with previous in vitro results, showing significant increases in mixed Smad complexes in two transgenic mouse models with tissue-specific overexpression of TGF-β1, as well as in mouse embryos (Heine et al. 1987) and human breast cancers (Figueroa et al. 2010) where endogenous TGF-β tends to be highly expressed.

Even though PLA is a very sensitive technique due to the RCA step, high-affinity antibodies are needed. When detecting protein-protein complexes, the two antibodies used must work with the same tissue pretreatment and antibody incubation conditions. Identifying useful antibodies becomes even more challenging when using the standard Duolink technology, as the two antibodies must be raised in different species. Given the strong PLA signal generated when our rabbit anti-Smad2/3 and anti-Smad1/5/9 antibodies are used individually (Fig. 2E), we were surprised at the relatively small number of canonical and mixed Smad complexes that were detected. However, there are a number of reasons why this might be the case. First, the relative geometry of the two different antibodies may be suboptimal in the context of the Smad complexes containing both targets, when compared with using either antibody alone to detect its cognate target. Second, antibody affinity may be an issue. Detection of canonical TGF-β and BMP Smad complexes is accomplished by using either our rabbit anti-Smad2/3 or anti-Smad1/5/9 in combination with a commercially available mouse anti-Smad4. We are seeking higher affinity Smad4 antibodies for future studies in order to increase the sensitivity of the PLA approach. Finally, we also found that more signal is seen when using primary antibodies in conjunction with oligonucleotide-conjugated secondary antibodies than with primary antibodies directly conjugated to the oligonucleotides. The secondary antibodies may decrease steric hindrance to allow for better amplification of signal. We may be able to increase the signals for mixed Smad complexes by finding antibodies from another species to detect the mixed Smad complexes using the secondary antibody protocol. More Smad complexes can be

detected using higher concentrations of primary antibody, but we have kept the antibody concentrations relatively low to keep background to a minimum. Using the conditions presented here, virtually no RCA products are detected over non-cellular areas of the section. Additionally, antibody concentrations should be low enough to allow for signals to be visualized as discreet dots to facilitate quantitation. Overall, we conclude that we can accurately compare relative levels of any given Smad complex between different tissues, but that we cannot accurately determine the relative representation of different Smad complexes within the same tissue because of the different detection efficiencies for the different complexes.

We developed the PLA methodology for use with FFPE tissues in order to analyze routinely processed patient samples and archival material. Indeed, the method has worked on a human breast tumor specimen (Fig. 6), and with a breast cancer TMA (Fig. 7). A recent report (Barros et al. 2014) used PLA to examine HER receptor dimerization in a TMA of breast cancers with overexpression of HER2. We also developed a brightfield read-out that generates a stable signal and allows for the simultaneous observation of the tissue histopathology. We did encounter some unexpected challenges in the development of this method. Early during method development, we observed some inconsistencies in the number and size of RCA products when similar samples were analyzed in different experiments. We occasionally observed a background "blush" in some tissue types, which could adversely affect the contrast between the RCA product and the tissue (see Fig. 3J and 3M for examples). Extending the time in ethanol post-staining to reduce this "blush" effect resulted in the loss of signal due to the solubility of Nova Red in aqueous ethanol. Keeping the substrate development time at 10 min and maintaining a consistent, reduced time in ethanol while dehydrating the slides were able to help decrease the background. We also saw more consistent results using a hematoxylin counterstain that did not require "blueing", as the time in running water also caused a decrease in the signal. We favored a light counterstain, because a dark counterstain can obscure the signal.

For these initial studies, we developed antibodies that would recognize all TGF-β Smads (Smads 2/3) and all BMP Smads (Smads1/5/9), as we did not know which individual Smads might be involved in generating the mixed Smad complex. A recent publication (Gronroos et al. 2012) suggests that phosphorylated Smad1/5-Smad3 is the major mixed Smad complex formed in multiple cell lines in vitro, and that this complex binds to BMP-responsive elements and mediates TGF-β-induced transcriptional repression of BMP target genes. In light of this result, we can attempt to find individual Smad2- and Smad3-specific antibodies that are suitable for PLA and try to reproduce these findings in tissue sections. Even though we have referred to the Smad2/3-Smad4 complexes as signaling intermediates of the canonical TGF-β pathway, it should be noted that other ligands in the TGF-superfamily, such as activin and nodal, also signal through the Smad 2/3-Smad 4 complex (Wakefield and Hill 2013). The ability of alternate ligands to induce formation of mixed Smad complexes remains to be determined. A recent report (Holtzhausen et al. 2014) showing that in vitro BMP2 can phosphorylate Smad2 and -3 in tumor cells suggests the possibility that ligands in the BMP/GDF branch of the superfamily may also induce formation of mixed Smad complexes. Thus, our approach may be broadly useful in querying signaling downstream of many members of the TGF-β superfamily.

More mixed than canonical Smad complexes were detected in many tissues of the mouse embryo whereas the opposite pattern was seen in normal adult mouse tissues where canonical signaling complexes predominate over mixed complexes. Canonical TGF-β Smad complexes may be more involved in mediating normal physiological homeostasis whereas mixed Smad complexes are preferentially induced during development or in disease processes where locally higher levels of TGF-β are present. Supporting this idea, along with the concept that carcinogenesis often recapitulates development (Nery 1976), mixed Smad signaling complexes are induced in human breast tumor samples and tumor xenografts, with little mixed Smad signaling observed in normal mammary ductal epithelium. This supports the data from cell culture studies where mixed Smad complexes mediated the signaling for TGF-β-induced anchorage-independent growth (Daly et al. 2008) and Smad1/5 phosphorylation was necessary for TGF-β-stimulated cell migration (Bharathy et al. 2008; Liu et al. 2009). Both of these biological activities are important in the carcinogenic process. As both canonical and mixed Smad complexes are observed in tumors, a more detailed analysis of the cell types expressing each of the Smad signaling complexes may provide clues as to the biological processes mediated by each of the Smad signaling complexes in vivo. For example, PLA using immunofluorescence has revealed an increase in Smad2/Smad4 and Smad3/Smad4 complexes in and around blood vessels in grade IV human gliomas as compared to control tissue (Dieterich et al. 2012). Mixed Smad complexes were not examined, but doing so might suggest whether canonical TGF-β Smad or mixed Smad signaling is more prominent in tumor-associated angiogenesis.

Additionally, we developed a method to automatically quantitate the brightfield signal present in tumor cells in the breast cancer TMA cores and demonstrated its utility on the test TMAs. This will allow easier quantitation of the various Smad complexes when analyzed in full-scale TMAs. In the analysis of our test TMA, ~40% of the cores that were able to be analyzed showed significant expression of mixed Smad complexes in tumor cells and the majority of these

were in cores that also expressed canonical BMP- and TGF-β Smad complexes. Approximately one third of the cores showed canonical BMP- and TGF-β Smad complexes without significant numbers of mixed Smad complexes. Additionally, in about 25% of the cores, only canonical BMP Smad complexes predominated, confirming the important role of BMPs in breast cancer (Alarmo et al. 2007; Ye et al. 2009). Correlating Smad complex formation with histopathological and clinical parameters may provide insight into the mechanistic actions of each Smad complex in different tumor types, and the quantitative assessment of the various complexes may generate useful predictive or pharmacodynamic biomarkers for ongoing trials with therapeutic TGF-β antagonists (Akhurst and Hata 2012).

A shift from canonical to mixed Smad signaling may accompany certain pathologies, and our preliminary data suggest this may be the case in breast cancer and in experimental fibrosis. We hope that using PLA to detect and quantitate Smad signaling complexes in patient samples (Blokzijl et al. 2010) will provide insight into the mechanism of disease progression and allow for the analysis of the potential efficacy of various treatment strategies.

Declaration of Conflicting Interests

The authors declared no potential conflicts of interest with respect to the research, authorship, and/or publication of this article.

Funding

The authors disclosed receipt of the following financial support for the research, authorship, and/or publication of this article: This research was supported by the Intramural Research Program of the NIH, NCI.

References

Akhurst RJ, Hata A (2012). Targeting the TGFbeta signalling pathway in disease. Nat Rev Drug Discov 11:790-811.

Alarmo EL, Kuukasjarvi T, Karhu R, Kallioniemi A (2007). A comprehensive expression survey of bone morphogenetic proteins in breast cancer highlights the importance of BMP4 and BMP7. Breast Cancer Res Treat 103:239-246.

Barros FF, Abdel-Fatah TM, Moseley P, Nolan CC, Durham AC, Rakha EA, Chan S, Ellis IO, Green AR (2014). Characterisation of HER heterodimers in breast cancer using in situ proximity ligation assay. Breast Cancer Res Treat 144:273-285.

Bharathy S, Xie W, Yingling JM, Reiss M (2008). Cancer-associated transforming growth factor beta type II receptor gene mutant causes activation of bone morphogenic protein-Smads and invasive phenotype. Cancer Res 68:1656-1666.

Blobe GC, Schiemann WP, Lodish HF (2000). Role of transforming growth factor beta in human disease. N Engl J Med 342:1350-1358.

Blokzijl A, Friedman M, Ponten F, Landegren U (2010). Profiling protein expression and interactions: proximity ligation as a tool for personalized medicine. J Intern Med 268:232-245.

Daly AC, Randall RA, Hill CS (2008). Transforming growth factor beta-induced Smad1/5 phosphorylation in epithelial cells is mediated by novel receptor complexes and is essential for anchorage-independent growth. Mol Cell Biol 28:6889-6902.

Dieterich LC, Mellberg S, Langenkamp E, Zhang L, Zieba A, Salomaki H, Teichert M, Huang H, Edqvist PH, Kraus T, Augustin HG, Olofsson T, Larsson E, Soderberg O, Molema G, Ponten F, Georgii-Hemming P, Alafuzoff I, Dimberg A (2012). Transcriptional profiling of human glioblastoma vessels indicates a key role of VEGF-A and TGFbeta2 in vascular abnormalization. J Pathol 228:378-390.

Feng XH, Derynck R (2005). Specificity and versatility in TGF-beta signaling through Smads. Annu Rev Cell Dev Biol 21:659-693.

Figueroa JD, Flanders KC, Garcia-Closas M, Anderson WF, Yang XR, Matsuno RK, Duggan MA, Pfeiffer RM, Ooshima A, Cornelison R, Gierach GL, Brinton LA, Lissowska J, Peplonska B, Wakefield LM, Sherman ME (2010). Expression of TGF-beta signaling factors in invasive breast cancers: relationships with age at diagnosis and tumor characteristics. Breast Cancer Res Treat 121:727-735.

Goumans MJ, Valdimarsdottir G, Itoh S, Rosendahl A, Sideras P, ten Dijke P (2002). Balancing the activation state of the endothelium via two distinct TGF-beta type I receptors. EMBO J 21:1743-1753.

Gronroos E, Kingston IJ, Ramachandran A, Randall RA, Vizan P, Hill CS (2012). Transforming growth factor beta inhibits bone morphogenetic protein-induced transcription through novel phosphorylated Smad1/5-Smad3 complexes. Mol Cell Biol 32:2904-2916.

Hall BE, Zheng C, Swaim WD, Cho A, Nagineni CN, Eckhaus MA, Flanders KC, Ambudkar IS, Baum BJ, Kulkarni AB (2010). Conditional overexpression of TGF-beta1 disrupts mouse salivary gland development and function. Lab Invest 90:543-555.

Heine U, Munoz EF, Flanders KC, Ellingsworth LR, Lam HY, Thompson NL, Roberts AB, Sporn MB (1987). Role of transforming growth factor-beta in the development of the mouse embryo. J Cell Biol 105:2861-2876.

Hill CS (2009). Nucleocytoplasmic shuttling of Smad proteins. Cell Res 19:36-46.

Hinck AP (2012). Structural studies of the TGF-betas and their receptors - insights into evolution of the TGF-beta superfamily. FEBS Lett 586:1860-1870.

Holtzhausen A, Golzio C, How T, Lee YH, Schiemann WP, Katsanis N, Blobe GC (2014). Novel bone morphogenetic protein signaling through Smad2 and Smad3 to regulate cancer progression and development. FASEB J 28:1248-1267.

Lehnert SA, Akhurst RJ (1988). Embryonic expression pattern of TGF beta type-1 RNA suggests both paracrine and autocrine mechanisms of action. Development 104:263-273.

Liu IM, Schilling SH, Knouse KA, Choy L, Derynck R, Wang XF (2009). TGFbeta-stimulated Smad1/5 phosphorylation requires the ALK5 L45 loop and mediates the pro-migratory TGFbeta switch. EMBO J 28:88-98.

Mozes MM, Bottinger EP, Jacot TA, Kopp JB (1999). Renal expression of fibrotic matrix proteins and of transforming growth factor-beta (TGF-beta) isoforms in TGF-beta transgenic mice. J Am Soc Nephrol 10:271-280.

Nery R (1976). Carcinogenic mechanisms: a critical review and a suggestion that oncogenesis may be adaptive ontogenesis. Chem Biol Interact 12:145-169.

Pelton RW, Dickinson ME, Moses HL, Hogan BL (1990). In situ hybridization analysis of TGF beta 3 RNA expression during mouse development: comparative studies with TGF beta 1 and beta 2. Development 110:609-620.

Sanderson N, Factor V, Nagy P, Kopp J, Kondaiah P, Wakefield L, Roberts AB, Sporn MB, Thorgeirsson SS (1995). Hepatic expression of mature transforming growth factor beta 1 in transgenic mice results in multiple tissue lesions. Proc Natl Acad Sci U S A 92:2572-2576.

Shi Y, Massague J (2003). Mechanisms of TGF-beta signaling from cell membrane to the nucleus. Cell 113:685-700.

Skliris GP, Parkes AT, Limer JL, Burdall SE, Carder PJ, Speirs V (2002). Evaluation of seven oestrogen receptor beta antibodies for immunohistochemistry, western blotting, and flow cytometry in human breast tissue. J Pathol 197:155-162.

Soderberg O, Gullberg M, Jarvius M, Ridderstrale K, Leuchowius KJ, Jarvius J, Wester K, Hydbring P, Bahram F, Larsson LG, Landegren U (2006). Direct observation of individual endogenous protein complexes in situ by proximity ligation. Nat Methods 3:995-1000.

Wakefield LM, Hill CS (2013). Beyond TGFbeta: roles of other TGFbeta superfamily members in cancer. Nat Rev Cancer 13:328-341.

Weibrecht I, Leuchowius KJ, Clausson CM, Conze T, Jarvius M, Howell WM, Kamali-Moghaddam M, Soderberg O (2010). Proximity ligation assays: a recent addition to the proteomics toolbox. Expert Rev Proteomics 7:401-409.

Wrighton KH, Lin X, Yu PB, Feng XH (2009). Transforming Growth Factor beta can stimulate Smad1 phosphorylation independently of Bone Morphogenetic Protein Receptors. J Biol Chem 284:9755-9763.

Ye L, Bokobza SM, Jiang WG (2009). Bone morphogenetic proteins in development and progression of breast cancer and therapeutic potential. Int J Mol Med 24:591-597.

Zieba A, Wahlby C, Hjelm F, Jordan L, Berg J, Landegren U, Pardali K (2010). Bright-field microscopy visualization of proteins and protein complexes by in situ proximity ligation with peroxidase detection. Clin Chem 56: 99-110.